



## Visualization of xenotransplanted human rhabdomyosarcoma after transfection with red fluorescent protein

Guido Seitz<sup>a,\*</sup>, Steven W. Warmann<sup>a</sup>, Jörg Fuchs<sup>a</sup>, Ulrike A. Mau-Holzmann<sup>e</sup>, Peter Ruck<sup>b</sup>, Heike Heitmann<sup>a</sup>, Robert M. Hoffman<sup>c</sup>, Jens Mahrt<sup>d</sup>, Gerhard A. Müller<sup>d</sup>, Johannes T. Wessels<sup>d</sup>

<sup>a</sup>Department of Pediatric Surgery, University Children's Hospital, 72076 Tübingen, Germany

<sup>b</sup>Institute of Pathology, Hospital Stuttgart-Leonberg, 71229 Leonberg, Germany

<sup>c</sup>AntiCancer Inc, San Diego, CA 92111, USA

<sup>d</sup>Department of Nephrology and Rheumatology, Center for Internal Medicine, 37075 Göttingen, Germany

<sup>e</sup>Department of Medical Genetics, Institute for Human Genetics, 72076 Tübingen, Germany

### Index words:

Rhabdomyosarcoma;  
Red fluorescent protein;  
Xenotransplantation

### Abstract

**Background/Aims:** *Discosoma sp* red fluorescent protein (DsRed2) is a newly developed marker for in vivo labeling studies in different biologic systems. After vector transfection, DsRed2 is expressed in mammalian cells and can be detected by fluorescence microscopy. The aims of this study were to establish a DsRed2-transfected human rhabdomyosarcoma (RMS) cell line and to perform a xenotransplantation on nude mice to use imaging as a tool for further basic research studies on this neoplasm.

**Procedure:** The human alveolar RMS cell line Rh30 was transfected with the pDsRed2-N1 vector by lipofection. The DsRed2-positive cells were sorted out by fluorescence-activated cell sorting analysis 96 hours after transfection and selected in culture with G418. Expression of DsRed2 messenger RNA was assessed using single-cell reverse transcriptase polymerase chain reaction after laser microdissection. Transfected and parental cells were characterized cytologically, cytogenetically, immunohistochemically, and in vivo after subcutaneous injection in NMRI (nu/nu) nude mice.

**Results:** After vector transfection, a pure and stable DsRed2-positive cell line was established by monoclonal growth of the cells. Reverse transcriptase polymerase chain reaction revealed constant expression of DsRed2 messenger RNA in fluorescing cells. There was no difference between transfected and parental cells by means of cell morphology and desmin expression. Clonal cells ( $1 \times 10^6$ ) were used for xenotransplantation. Tumors were visualized noninvasively through the skin of the mice using specific emission and excitation filters. Tumor vascularization and vessel growth could be discriminated from tumor tissue using this imaging system.

This article was presented at the 36th SIOP Meeting in Oslo from September 15 to 19, 2004.

\* Corresponding author. Tel.: +49 7071 2986621; fax: +49 7071 294046.

E-mail address: guido.seitz@med.uni-tuebingen.de (G. Seitz).

**Conclusion:** This is the first report on successful transfection of an RMS cell line with red fluorescent protein followed by xenotransplantation into nude mice. This model can serve as an imaging tool for *in vivo* studies investigating tumor biology and metastases of human RMS.

© 2006 Elsevier Inc. All rights reserved.

Rhabdomyosarcoma (RMS) is the most common soft tissue sarcoma in children. Approximately two thirds of all sarcomas and 7% to 8% of all solid malignant tumors in children are RMSs [1]. The 2 main histopathologic subtypes of this malignancy in children are embryonal and alveolar RMSs [2]. Specific genetic alterations [3] such as t(2;13)(q35;q14), which occurs in 55% of all cases, and t(1;13)(p36;q14), which occurs in 22%, contribute to the diagnosis of alveolar RMS [1]. No specific genetic alteration has been found in embryonal RMSs [1].

Many techniques have been used for investigating RMS in models. However, investigations on early-stage tumor behavior and development of metastasis are limited owing to lack of tumor visualization.

Red fluorescent protein (RFP) is a 25.7-kDa protein and a variant of naturally occurring chromoproteins found in colored body parts of corals and anemones—*Discosoma sp.* *Discosoma sp* RFP (DsRed2) was developed through a combination of random and site-directed mutageneses. *Discosoma sp* RFP was engineered using 3 amino-acid substitutions (V105A, I161T, and S197A) for a more rapid maturation as compared with wild-type RFP and 3 substitutions (R2A, K5E, and K9T) that prevent the protein from aggregating nonspecifically [4]. *Discosoma sp* RFP has an excitation peak at 561 nm and an emission maximum at 587 nm [5]. Transfection can be performed using the pDsRed2-N1 vector [6]. This vector is equipped with a neomycin resistance cassette, which confers a resistance against neomycin and therefore allows stable selection after transfection using G418. Transfected cells can be visualized using fluorescence microscopy [7], laser-scanning microscopy [8], and multiphoton laser-scanning microscopy [9]. Red fluorescent protein has already been used for investigating pancreatic cancer *in vivo* [10]. The aims of this study were to first establish a stable DsRed2-transfected RMS cell line and to then transplant transfected cells into nude mice to use imaging as a tool for visualizing tumor growth in real time.

## 1. Materials and methods

### 1.1. Cell line

The alveolar RMS cell line Rh30 (DSMZ, Braunschweig, Germany) was cultured in Dulbecco's modified eagle medium (DMEM) supplemented with 10% fetal calf serum, 4.5% L-Glu, and 2.5% HEPES in a humidified atmosphere containing 5% CO<sub>2</sub> at 37°C.

### 1.2. *Discosoma sp* RFP vector

The vector pDsRed2-N1 was purchased from BD Biosciences Clontech (Palo Alto, Calif). The vector encodes DsRed2, a variant of the *Discosoma sp* RFP. *Discosoma sp* RFP includes a series of silent base-pair changes resulting in higher expression in mammalian cells. A neomycin resistance cassette, consisting of the simian virus 40 early promoter and other signals, allows stably transfected eukaryotic cells to be selected using G418.

### 1.3. *Discosoma sp* RFP transfection

Transfection of the Rh30 cell line (RMS) was carried out by lipofection. A total of 200  $\mu$ L of OptiMEM (Gibco, Karlsruhe, Germany) and that of 5  $\mu$ L of Lipofectamine (Invitrogen, Karlsruhe, Germany) were incubated with 5  $\mu$ g of pDsRed2-N1 for 30 minutes at room temperature to form a Lipofectamine-vector complex. This complex was then added to Rh30 cells (in 6-well plates at  $1 \times 10^6$  cells per well) with incubation for 5 hours at 37°C. Transfection was stopped by adding 10% fetal calf serum in DMEM to the cells.

The transfection rate was determined after 24 hours using fluorescence microscopy (excitation = 561 nm; emission = 587 nm).

### 1.4. Selection of DsRed2-positive cells

The DsRed2-positive cells were sorted out by fluorescence-activated cell sorting analysis (FACSVantage SE, BD, Heidelberg, Germany) using a DsRed2 filter 96 hours after transfection. Cells were washed twice and resuspended in FACSFlo (BD). Flow cytometry was performed using nontransfected cells as negative control subjects. Original and transfected cells were analyzed with regard to their size and granularity. The DsRed2-positive cells were sorted out and selected when fluorescence intensity on the selected channel was higher than  $1 \times 10^2$ . The selected cells were immediately resuspended in DMEM as previously described and then selected by G418 (1.6 mg/mL). To establish a pure DsRed-positive cell line, we cloned transfected cells after selection.

### 1.5. *Discosoma sp* RFP messenger RNA detection in transfected cells

Single-cell reverse transcriptase polymerase chain reaction (RT-PCR) was used to detect DsRed2 messenger RNA (mRNA) after transfection. Cells were initially identified by fluorescence microscopy as described. Ten single cells were

identified and harvested by laser microdissection (PALM Robo, Software PALM Robo Version 1.21, Microlaser Technologies, Bernried, Germany) and then placed in mineral oil (Sigma, Steinheim, Germany) for further analysis.

Amplification of targeted mRNA was performed via one-step RT-PCR; GAPDH (glyceraldehyde-3-phosphate dehydrogenase) served as a housekeeping gene standard. A negative control cell with nontranscribed mRNA was used to demonstrate that no genomic DNA was amplified.

Messenger RNA was isolated from dissected cells using an Invisorb RNA Kit I 100 (No. 10601004, Invitex, Berlin, Germany). Complementary DNA transcription and single-cell PCR were performed in one step according to the Qiagen one-step RT-PCR protocol (No. 210212, Qiagen One-step RT-PCR Kit, Qiagen, Hilden, Germany). The reaction mix (20  $\mu$ L) consisted of 6.52  $\mu$ L of diethylpyr-carbonate water, 4  $\mu$ L of RT buffer 5 $\times$ , 4  $\mu$ L of Q-Solution, 0.8  $\mu$ L of deoxynucleotide triphosphate mix 10 mmol/L, 0.8  $\mu$ L of enzyme mix, 0.08  $\mu$ L of ribonuclease inhibitor, 0.4  $\mu$ L of forward primer, 0.4  $\mu$ L of reverse primer, and 3  $\mu$ L of template. Transcription of mRNA was performed by incubation for 35 minutes at 50°C. After a hot start (15 minutes at 95°C), PCR was carried out in 55 cycles. One cycle consisted of a denaturation step (60 seconds at 94°C), an annealing step (90 seconds at 56°C), and an elongation step (60 seconds at 72°C). Finally, a closing step was added (10 minutes at 72°C).

The following DsRed2 amplifiers were chosen: sense 5'-CTG TCC CCC CAG TTC CAG TAC-3' and antisense 5'-CGT TGT GGG AGG TGA TGT CCA GCT-3' (435 base pairs).

The following GAPDH amplifiers were used: sense 5'-CCC TTC ATT GAC CTC AAC TAC-3' and antisense 5'-TGA GTC CTT CCA CGA TAC C-3' (418 base pairs).

### 1.6. Cytologic analysis of transfected and nontransfected cells

Cytologic analysis of the transfected and nontransfected cell lines was performed by a pathologist (PR). Cells were grown on microscopic slides and hematoxylin-eosin staining was performed. Cytologic analysis was carried out by light microscopy using high-power fields (400 $\times$ ).

### 1.7. Cytogenetic analysis of transfected and nontransfected cells

A cytogenetic analysis of the nontransfected and transfected cell lines was performed. Therefore, both cell lines were grown and harvested under equal conditions according to standard protocols [11].

### 1.8. Transplantation of transfected tumor cells to nude mice

Transfected cells were cloned as previously described. One week before transplantation, G418 selection was removed and cells were maintained in the described culture

medium. Approximately 10<sup>6</sup> tumor cells (2 mL) were injected subcutaneously in the right flank of 6- to 8-week-old female nude mice (NMRI nu/nu, MH Hanover, Hanover, Germany).

### 1.9. Visualization of subcutaneously growing tumors

Animals were anesthetized by inhalation of ether. For in vivo visualization, a cold light source (KL 1500, Schott, Mainz, Germany) was used with a green excitation filter (HQ 535, Chroma Technology Corp. Rockingham, VT) and a red emission filter (OG 590 LP, Chroma USA).

### 1.10. In vivo growth pattern of transfected and nontransfected tumors

Transplanted animals were continuously observed and clinically examined. Tumor volumes were measured every 5 days with a caliper (a indicates length; b, width; c, height). Tumor volumes were calculated using the following formula:  $a/2 \times b/2 \times c/2 \times 4/3\pi$ . Overall observation time was up to 30 days, depending on tumor size.

Relative tumor volumes were calculated using the following formula:  $V_{rel} = V_{dx}/V_{d0}$ , with  $V_{dx}$  being the tumor volume on day  $x$  and  $V_{d0}$  being the tumor volume at the beginning of the observation time. Both groups (with transfected and nontransfected tumors) consisted of 8 animals. Mean values and standard deviations were calculated and statistically analyzed in both groups using Student's  $t$  test.

### 1.11. Histologic analysis of transfected and nontransfected tumors

After reaching a volume of 0.5 cm<sup>3</sup>, tumors were resected under general anesthesia. Tissue was fixed in formalin (37%) and processed for histologic analysis. Hematoxylin-eosin staining (3- $\mu$ m slides) of the transfected and nontransfected tumors was performed. The slides were analyzed for changes in histology, mitotic rate, and necrosis using high-power fields (400 $\times$ ).

### 1.12. Immunotyping by desmin immunohistochemistry

For immunotyping, desmin immunohistochemistry was performed. Tissue was processed as previously mentioned and prepared for fluorescence immunohistochemistry (3- $\mu$ m slides). Sections were first deparaffinized by xylene and ethanol (xylene, 3  $\times$  5 minutes; ethanol 99.9%, 2  $\times$  10 minutes; ethanol 96%, 2  $\times$  10 minutes). After antigen demasking with 10 mmol/L of citrate buffer (pH 6.0, 2 minutes at 100 °C followed by 20 minutes at room temperature) and blocking of unspecific backgrounds by 1.5% goat serum (Dako, Hamburg, Germany) for 30 minutes, the primary monoclonal mouse antihuman desmin clone D33 (dilution, 1:100; Dako) was added for 120 minutes. After triple phosphate-buffered saline (PBS)



**Fig. 1** Fluorescence microscopy showing DsRed2-positive RMS cells after transfection (Rh30 cell line, original magnification  $\times 400$ ).

washing, the secondary antibody Cy3 (goat antimouse; dilution, 1:300; Dianova, Hamburg, Germany) was added for 30 minutes. After triple PBS washing, a counterstaining with Dapi (dilution, 1:10,000; D9542, Sigma-Aldrich, Munich, Germany) was performed. Slides were washed

again 3 times with PBS and embedded with a mounting medium (Sigma-Aldrich).

The slides were analyzed for desmin expression by fluorescence microscopy using high-power fields ( $400\times$ ).

All animal studies were approved by the regional government's ethical committee for animal studies (Tübingen, Germany).

## 2. Results

The transfection rate of DsRed2 in RMS cells was approximately 55% after 24 hours. Transfected cells could be visualized by fluorescence microscopy (excitation = 561 nm; emission = 587 nm; Fig. 1).

Fluorescence-activated cell sorting analysis showed the standard deviation of RMS cells (cell size vs granularity). No significant difference in cell size and granularity between nontransfected and transfected cells could be observed. Analysis of fluorescence on the DsRed2 channel revealed a correlating population of transfected cells with a fluorescence intensity greater than  $10^2$ . In nontransfected cells, no fluorescence was observed. After positioning of the respective gate, highly positive DsRed2 cells were identified and sorted out (Fig. 2).

Single-cell RT-PCR after laser microdissection revealed a stable expression of DsRed2 mRNA in fluorescent cells.

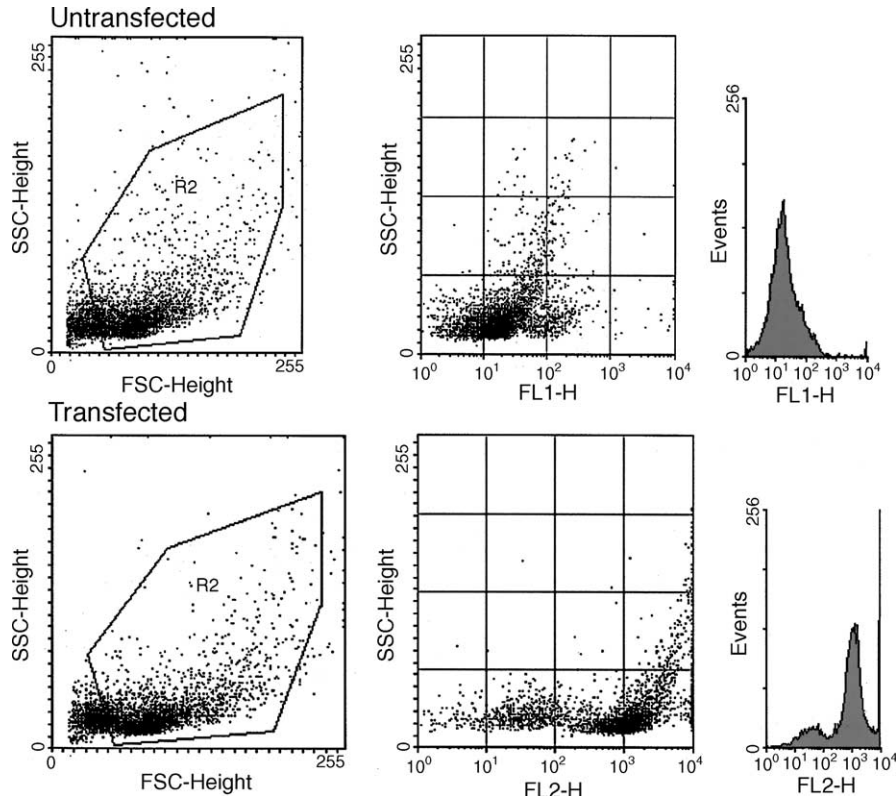


**Fig. 2** Fluorescence-activated cell sorting analysis of the Rh30 cell line (fluorescein isothiocyanate vs size) showing a pure fluorescing population in transfected cells as compared with nontransfected cells.

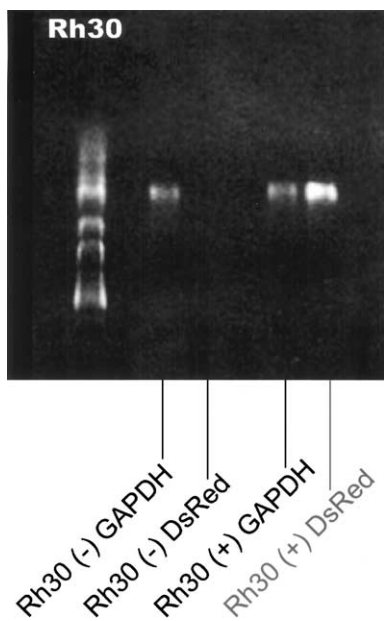


**Fig. 3** Single-cell RT-PCR after laser microdissection revealing constant expression of DsRed2 mRNA.

*Discosoma sp* RFP expression in nontransfected cells was negative (Fig. 3).

Cell division rates were identical in both transfected and nontransfected lines. The population doubling time was 4 days in both cultures (data not shown).

Cytogenetic analysis of the tumor cells showed a translocation, t(2;13), in transfected and nontransfected cells, which was described originally in the Rh30 cell line [12]. Other frequent abnormalities found in the near-tetraploid cell lines (nontransfected and transfected) included complex rearrangements of chromosomes 1 and 9, such as [i(1q), i(1p), i(9q)].

Subcutaneously growing tumors could be detected in the right flank of the animals by fluorescence (Fig. 4). Tumor visualization was possible immediately after transplantation. In contrast, tumors could be detected for the first time macroscopically 7 days later and could then be followed for

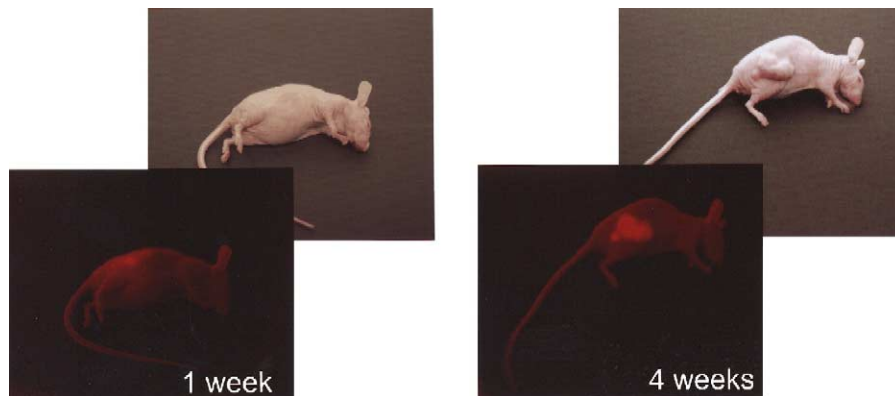


**Fig. 4** Left panel shows visualization of DsRed2-positive alveolar RMS in nude mice (NMRI nu/nu) 1 week after xenotransplantation in which the tumor was not visible macroscopically; right panel, visualization of the same tumor as that on the left panel after 4 weeks of tumor growth (fluorescent image/nonfluorescent image).

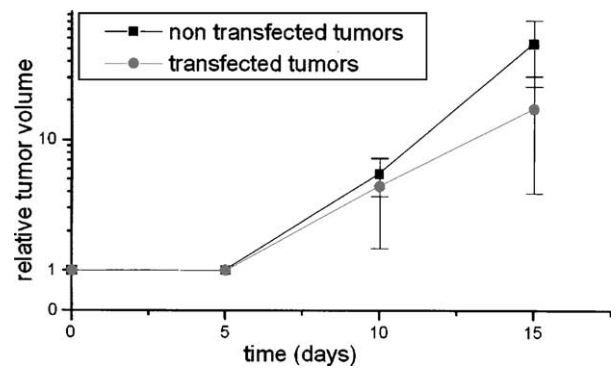


**Fig. 5** Relative tumor volumes showing no significant difference in tumor growth between transfected and nontransfected tumors.

4 weeks. Analysis of growth rates showed no significant difference in growth behavior between transfected RMS and control tumors (Fig. 5). Standard histology (hematoxylin-eosin staining) revealed similar morphologies of transfected and nontransfected cells announcing a highly malignant sarcoma. Evaluation of mitosis rate showed a rate that was greater than 20 mitoses per high-power field in transfected and nontransfected tumors. The extent of necrosis differed from tumor to tumor and did not depend on DsRed2 expression (Fig. 6A and B). Desmin fluorescence immunohistochemistry showed no difference in the expression of desmin in transfected and nontransfected subcutaneously growing tumor cells (Fig. 7A and B).

### 3. Discussion

Rhabdomyosarcoma is the most common soft tissue sarcoma in children [13]. The prognosis of these tumors is still sobering [14]. The main clinical treatment problems are local tumor recurrence, lymph node metastases in alveolar RMS, and low survival rates in advanced tumors [15]. Lymph node metastases can only be detected by computed tomographic scan, magnetic resonance imaging, and ultrasound examination. Residual tumor evaluation after chemo-

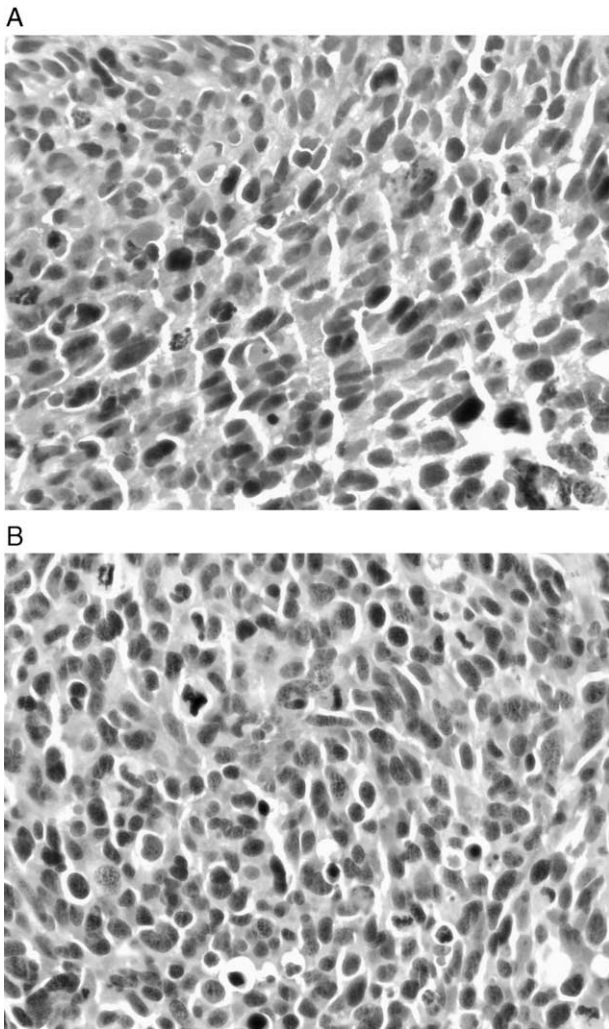


**Fig. 6** A, Hematoxylin-eosin staining (original magnification  $\times 40$ ) of tumor specimen from the Rh30 cell line without transfection showing a typical small blue cell tumor. B, Hematoxylin-eosin staining (original magnification  $\times 40$ ) of tumor specimen from the Rh30 cell line with DsRed2 transfection showing no difference in histology as compared with the outcome discussed in panel A.

therapy can only be performed by second-look surgical procedures. The absence of tumor markers requires a response evaluation by tumor size. Another problem is the necessity of mutilating surgical procedures (eg, amputation of extremities, enucleation of an eye, exstirpation of the bladder or rectum) [2]. Visualization of childhood RMS would offer new opportunities in the evaluation of tumor response and provide new tools for nonmutilating surgical procedures under maintenance of safety margins.

Fluorescent proteins are important tools for further *in vitro* and *in vivo* visualization studies. Enhanced green fluorescent protein (GFP) was the first fluorescing protein described in biologic systems and was used to evaluate myofibrillogenesis in living cells [16], as well as in treatment procedures in cell lines [17].

In mouse models of cancer, fluorescent proteins have enabled visualization of orthotopically growing tumors and resulting metastases [18]. For example, GFP has been used for real time optical imaging of primary tumor growth and metastasis in pancreatic cancer [19]. Real time imaging of fibrosarcoma lung metastases through GFP has also been described already [20]. Bone and lung metastases of human breast cancer could be visualized using GFP in an animal model [21,22]. Tanaka et al [23] described GFP-expressing cells in voided urine found only in animals with developing bladder cancer. This model now serves as a noninvasive detection method for bladder cancer [23]. There are also reports on GFP-labeled cell lines in colon cancer to enable visualization of liver metastases [24]. Katz et al [25] used GFP for gene therapy of pancreatic cancer by induction of apoptosis via the tumor necrosis factor-related apoptosis-inducing ligand.

Red fluorescent protein (DsRed2) is a recently developed tool for oncological research. Because of its longer

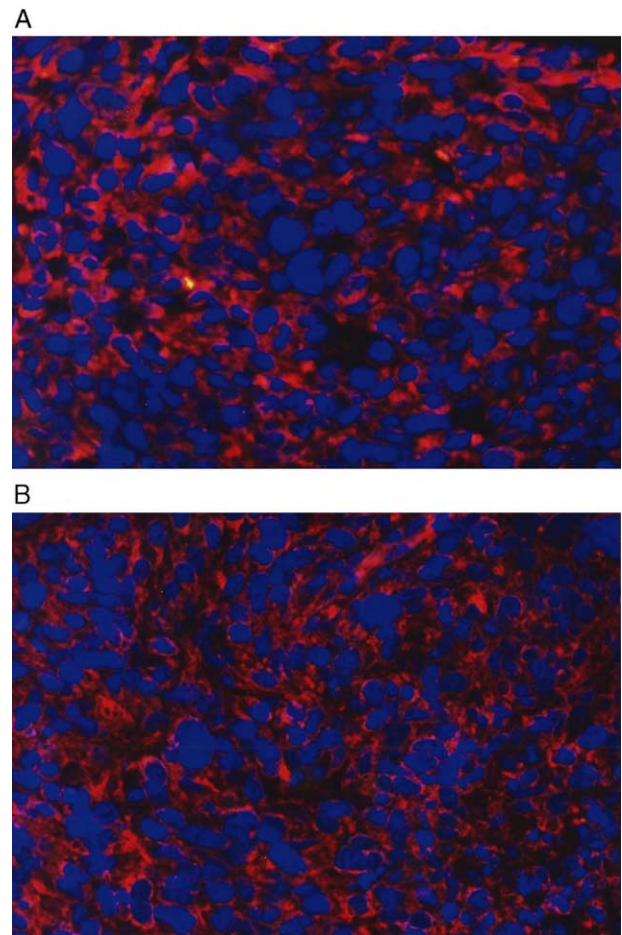


**Fig. 7** A, Desmin immunohistochemistry with fluorescence microscopy from the Rh30 cell line without transfection showing a desmin-expressing tumor (original magnification  $\times 40$ ). B, Desmin immunohistochemistry with fluorescence microscopy from the Rh30 cell line after transfection showing a desmin-expressing tumor (original magnification  $\times 40$ ).

wavelength and lower energy emission, RFP transmits more efficiently through whole tissue as compared with green emitters and is better distinguishable from background fluorescence [26]. Katz et al [27] reported on successful real time assessment of chemotherapy efficacy in an orthotopic pancreatic cancer model using the RFP. Lu et al [28] described detection and investigation of physiologic patterns of cancer invasion and metastases in cervical cancer in vivo using DsRed2. A combination of GFP and DsRed2 transfection was performed to evaluate metastatic growth patterns of 2 differently color-encoded sublines from a human fibrosarcoma in a mouse model to determine the clonality of metastasis [29,30]. Another methodological approach in dual-color fluorescence is the use of RFP-expressing tumors growing in GFP-expressing transgenic mice. In this model, tumor-host interactions by whole-body imaging can be visualized [31].

We successfully performed transfection of human RMS with RFP and transplantation of transfected cells into nude mice (NMRI nu/nu). A successful transfection of hepatoblastoma with GFP by lipotransfection was recently described by our group [32]. With this model, other fluorescent proteins could be transfected as well.

We used Rh30 cells with adherent cell layers after liposomal transfection. Interestingly, the initial transfection rate in the Rh30 cell line (55%) after liposomal transfection was much higher than the transfection rates reported in earlier studies [18,32].

Cell selection by flow cytometry and G418 resistance is necessary to obtain a stable transfected cell line. This selection prevents an overgrowth of nonfluorescent cells that did not undergo transfection [32].

Growth behavior, histology, and mitotic rates were similar in transfected and nontransfected tumors. There was no significant difference in tumor volumes. Rate of necrosis differed from tumor to tumor and depended on tumor size, not on expression of DsRed2. There was no difference in desmin expression between transfected and nontransfected cells. Cytogenetic analysis lines revealed translocations and chromosomal abnormalities in both cells with rearrangement of chromosomes. Therefore, transfection of these tumors with DsRed2 did not lead to a change in their biologic behavior. Further studies will be carried out comparing parental and transfected cells.

Tumors were visualized immediately after xenotransplantation, and their development was monitored in real time even if they were not visible macroscopically. This observation contradicts that of Libutti et al, who claimed that a waiting period of 7 days after transplantation was necessary to visualize GFP-mediated tumor fluorescence [33]. In addition, tumor volumes can be measured much easily by fluorescence than with calipers.

Fluorescent proteins might serve as an innovative basis for further studies on childhood sarcomas analyzing angiogenesis, anticancer drug efficacy, and tumor-host interactions. Clinical implications include detection of

primary tumors, recurrences, and metastases, as well as nonmutilating intraoperative procedures. Such clinical applications of fluorescent proteins in neoplasms have been already reported for glioblastomas and bladder carcinomas [34-36].

## Acknowledgment

We thank Hannes Schramm (Department of Photography, University Hospital Tübingen, Tübingen, Germany) for his support.

## References

- [1] McDowell HP. Update on childhood rhabdomyosarcoma. *Arch Dis Child* 2003;88:354-7.
- [2] Pappo AS, Shapiro DN, Crist WM, et al. Biology and therapy of pediatric rhabdomyosarcoma. *J Clin Oncol* 1995;13:2123-9.
- [3] Sorensen PHB, Lynch JC, Qualman SJ, et al. *PAX3-FKHR* and *PAX7-FKHR* gene fusions are prognostic indicators in alveolar rhabdomyosarcoma: a report from Children's Oncology Group. *J Clin Oncol* 2002;20:2672-9.
- [4] Yarbrough D, Wachter RM, Kallio K, et al. Refined crystal structure of DsRed, a red fluorescent protein from coral, at 2.0-Å resolution. *Proc Natl Acad Sci U S A* 2001;98:462-7.
- [5] Bevis BJ, Glick BS. Rapidly maturing variants of the *Discosoma* red fluorescent protein (DsRed). *Nat Biotechnol* 2002;20:83-7.
- [6] Matz MV, Fradkov AF, Labas YA, et al. Fluorescent proteins from nonbioluminescent Anthozoa species. *Nat Biotechnol* 1999;17:969-73.
- [7] Ausubel FM, Brent R, Kingston RE, et al. *Current protocols in molecular biology*, vol. 1. New York: John Wiley and Sons; 1994 [Ch. 5 and 9].
- [8] Hawley TS, Telford WG, Ramezani A, et al. Four-color flow cytometric detection of retrovirally expressed red, yellow, green and cyan fluorescent protein. *Biotechniques* 2001;30:1028-34.
- [9] Jakobs S, Subramaniam V, Schonle A, et al. EFGP and DsRed expressing cultures of *Escherichia coli* imaged by confocal, two-photon and fluorescence lifetime microscopy. *FEBS Lett* 2000;479:131-5.
- [10] Katz MH, Bouvet M, Takimoto S, et al. Selective antimetastatic activity of cytosine analog CS-682 in a red fluorescent protein orthotopic model of pancreatic cancer. *Cancer Res* 2003;63:5521-5.
- [11] Wegner R.D. Editor. *Diagnostic cytogenetics*. Springer lab manual. Berlin, Germany: Springer; 1999. p. 239-40.
- [12] Douglass EC, Valentine M, Etcubanas E, et al. A specific chromosomal abnormality in rhabdomyosarcoma. *Cytogenet Cell Genet* 1987;45(3-4):148-55.
- [13] Prados J, Melguizo C, Marchal JA, et al. Therapeutic differentiation in human rhabdomyosarcoma cell line selected for resistance to actinomycin D. *Int J Cancer* 1998;75:379-83.
- [14] Newton WA, Soule EH, Hamoudi AB, et al. Histopathology of childhood sarcomas, Intergroup Rhabdomyosarcoma Studies I and II: clinicopathological correlation. *J Clin Oncol* 1988;6:67-75.
- [15] Cocker HA, Pinkerton CR, Kelland LR. Characterization and modulation of drug resistance of human pediatric rhabdomyosarcoma cell lines. *Br J Cancer* 2000;83(3):338-45.
- [16] Dabiri GA, Ayoob JC, Turmacioglou KK, et al. Use of GFP linked to cytoskeletal proteins to analyse myofibrillogenesis in living cells. *Methods Enzymol* 1999;302:171-86.

- [17] Hunt L, Batard P, Jordan M, et al. Fluorescent proteins in animal cells for process development: optimization of sodium butyrate treatment as an example. *Biotechnol Bioeng* 2002;77:528-37.
- [18] Hoffman RM. Green fluorescent protein imaging of tumour growth, metastasis, and angiogenesis in mouse models. *Lancet Oncol* 2002;3:546-52.
- [19] Bouvet M, Wang JW, Nardin SR, et al. Real time optical imaging of primary tumor growth and multiple metastatic events in pancreatic cancer orthotopic model. *Cancer Res* 2002;62:1534-40.
- [20] Yamamoto M, Yang M, Jiang P, et al. Real time GFP imaging of spontaneous HT-1080 fibrosarcoma lung metastases. *Clin Exp Metastasis* 2003;20:181-5.
- [21] Zhang JH, Tang J, Wang J, et al. Over-expression of bone sialoprotein enhances bone metastasis of human breast cancer cells in a mouse model. *Int J Oncol* 2003;23(4):1043-8.
- [22] Goodison S, Kawai K, Hihara J, et al. Prolonged dormancy and site-specific growth potential of cancer cells spontaneously disseminated from nonmetastatic breast tumors as revealed by labeling with green fluorescent protein. *Clin Cancer Res* 2003;9:3808-14.
- [23] Tanaka M, Gee JR, De la Cerda J, et al. Noninvasive detection of bladder cancer in an orthotopic murine model with green fluorescent protein cytology. *J Urol* 2003;170:975-8.
- [24] Sturm JW, Keese MA, Petruch B, et al. Enhanced green fluorescent protein-transfection of murine colon carcinoma cells: key for early tumor detection and quantification. *Clin Exp Metastasis* 2003;20(5):395-405.
- [25] Katz MH, Spivack DE, Takimoto S, et al. Gene therapy of pancreatic cancer with green fluorescent protein and tumor necrosis factor-related apoptosis-inducing ligand fusion gene expression driven by a human telomerase reverse transcriptase promoter. *Ann Surg Oncol* 2003;10(7):762-72.
- [26] Baird GS, Zacharias DA, Tsien RY. Biochemistry, mutagenesis, and oligomerization of DsRed, a red fluorescent protein from coral. *Proc Natl Acad Sci U S A* 2000;97(22):11984-9.
- [27] Katz MH, Takimoto S, Spivack D, et al. A novel red fluorescent protein orthotopic pancreatic cancer model for the preclinical evaluation of chemotherapeutics. *J Surg Res* 2003;113(1):151-60.
- [28] Lu JY, Chen HC, Chu RY, et al. Establishment of red fluorescent protein-tagged HeLa tumor metastasis models: determination of DsRed2 insertion effects and comparison of metastatic patterns after subcutaneous, intraperitoneal, or intravenous injection. *Clin Exp Metastasis* 2003;20(2):121-3.
- [29] Yamamoto N, Yang M, Jiang P, et al. Real-time imaging of individual fluorescent-protein color-coded metastatic colonies in vivo. *Clin Exp Metastasis* 2003;20(7):633-8.
- [30] Yamamoto N, Yang M, Jiang P, et al. Determination of clonality of metastasis by cell-specific color-coded fluorescent-protein imaging. *Cancer Res* 2003;63:7785-90.
- [31] Yang M, Li P, Jiang L, et al. Dual-color fluorescence imaging distinguishes tumor cells from induced angiogenic vessels and stromal cells. *Proc Natl Acad Sci U S A* 2003;100(24):14259-62.
- [32] Warmann SW, Fuchs J, Seitz G, et al. New trends in tumor biology: transfection of a human hepatoblastoma cell line with green fluorescent protein. Accepted for publication. *J Pediatr Surg*.
- [33] Choy G, O'Connor S, Diehn FE, et al. Comparison of noninvasive fluorescent and bioluminescent small animal optical imaging. *Bio-techniques* 2003;35(5):1022-6, 1028-30.
- [34] Stummer W, Novotny A, Stepp H, et al. Fluorescence-guided resection of glioblastoma multiforme by using 5-aminolevulinic acid-induced porphyrins: a prospective study in 52 consecutive patients. *J Neurosurg* 2000;93(6):1003-13.
- [35] Riesenber R, Fuchs C, Kriegmair M. Photodynamic effects of 5-aminolevulinic acid-induced porphyrin on human bladder carcinoma cells in vitro. *Eur J Cancer* 1996;32A(2):328-34.
- [36] Engbrecht BW, Menon C, Kachur AV, et al. Photofrin-mediated photodynamic therapy induces vascular occlusion and apoptosis in a human sarcoma xenograft model. *Cancer Res* 1999;59:4334-42.